

Contribution from the Departments of Chemistry, Texas A&M University, College Station, Texas 77843, and University of Delaware, Newark, Delaware 19716

Carbon Dioxide Insertion Processes Involving Metal-Carbon Bonds: Solid-State and Solution Structure of [Na(18-crown-6)][W(CO)₅CH₃]

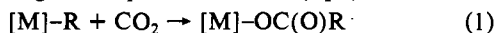
Donald J. Darensbourg,*† Christopher G. Bauch,† and Arnold L. Rheingold*‡

Received August 11, 1986

Carbon dioxide insertion reactions into the CH₃-W bonds of *cis*-CH₃W(CO)₄L⁻ derivatives (L = CO or phosphorus donor ligands) to afford the corresponding acetato complexes have provided mechanistic insight concerning this C-C bond-forming process. When L = PMe₃, the insertion reaction was found to occur about 250 times faster than when L = CO. Relevant to these insertion reactions, the structure of [Na(18-crown-6)(THF)₂][CH₃W(CO)₅] has been established by X-ray crystallography, and a comparison is made with the phosphine-substituted derivative. The compound crystallizes in the monoclinic space group C2/c with cell dimensions *a* = 12.962 (2) Å, *b* = 12.607 (5) Å, *c* = 20.22 (1) Å, β = 91.76 (2)°, *V* = 3302.2 Å³, and *D*_{calcd} = 1.55 g cm⁻³ for *Z* = 4. The structure consists of an array of the two discrete ionic units at normal van der Waals distances, where the Na⁺ is octacoordinated and the tungsten metal is in an octahedral environment. The W-CH₃ bond distance at 2.313 (17) Å is almost identical with that previously noted in the isoelectronic neutral rhenium analogue CH₃Re(CO)₅, and is longer than that found in *cis*-CH₃W(CO)₄PMe₃⁻. Although Na(18-crown-6)⁺ is complexed by two tetrahydrofuran molecules in the solid-state structure, these ligands are necessarily labile in THF solution. This is manifested in the observation that Na(18-crown-6)(THF)₂⁺ behaves in much the same manner as Na(THF)_{*n*}⁺ in enhancing the rate of carbon dioxide insertion into the W-CH₃ bond, a phenomenon ascribed to a neutralization of negative charge buildup on the incipient acetate ligand by the Na⁺ ion.

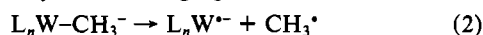
Introduction

In previous investigations we have endeavored to comprehend the mechanistic aspects operative in carbon-carbon bond-forming processes resulting from carbon dioxide insertion into metal-carbon bonds.¹⁻³ These studies have emphasized the use of anionic group 6 metal-alkyl and -aryl derivatives, e.g., CH₃W(CO)₅⁻, as substrates for probing this important reaction (eq 1).



Kinetic measurements have revealed significant rate enhancement for carbon dioxide insertion into the [W]-CH₃ linkage upon replacing an ancillary CO ligand with electron-donating phosphine ligands. That is, carbon dioxide insertion into the W-CH₃ bond of *cis*-W(CO)₄[PMe₃]₂CH₃⁻ occurs 250 times more rapidly than that of W(CO)₅CH₃⁻. This result was attributed to a greater interaction of CO₂ with the electron-rich metal center of *cis*-W(CO)₄[PMe₃]₂CH₃⁻ as opposed to a destabilization of the W-CH₃ bond in this species. Nevertheless, it is necessary to firmly establish the relationship between W-CH₃ bond strength and the nature of the ancillary ligands about the zerovalent tungsten.

There is in general a lack of structural or thermodynamic data for metal-carbon bonds in metal-alkyl and -aryl derivatives of zerovalent group 6 metals. Herein we report the X-ray structural analysis of [Na(18-crown-6)][W(CO)₅CH₃], for comparison with the available structural data for [PPN][*cis*-W(CO)₄(PMe₃)₂CH₃], in an effort to assess the relative metal-alkyl bond dissociation energies of these two species (18-crown-6 = 1,4,7,10,13,16-hexa-oxacyclooctadecane; PPN = bis(triphenylphosphine)nitrogen(1+)). That is, comparative W-CH₃ bond dissociation energies (*D*_{L,W-R}) as a function of the nature of the ancillary ligands (L), corresponding to the endothermicity of the process defined by eq 2, should be correlatable with W-CH₃ bond distances in the absence of sterically encumbering ligands.



Experimental Section

All manipulations were carried out either in an argon drybox or on a double-manifold Schlenk vacuum line with use of tetrahydrofuran, which was dried by distillation from sodium-benzophenone ketyl under nitrogen. W(CO)₆ was purchased from Strem Chemicals, Inc., and methyl tosylate was acquired from Aldrich. 18-crown-6 (1,4,7,10,13,16-hexa-oxacyclooctadecane) was supplied by Aldrich Chemical Co. W(CO)₅NMe₃ was prepared from W(CO)₆ and

Table I. Crystal, Data Collection, and Refinement Parameters for [Na(18-crown-6)(THF)₂][CH₃W(CO)₅]

formula	C ₂₆ H ₄₃ O ₁₃ NaW	<i>Z</i>	4
cryst syst	monoclinic	μ, cm ⁻¹	37.6
space group	C2/c	color	yellow plates
<i>a</i> , Å	12.962 (6)	size, mm	0.20 × 0.15 × 0.08
<i>b</i> , Å	12.607 (5)	temp, °C	-88
<i>c</i> , Å	20.22 (1)		
β, deg	91.76 (2)	<i>D</i> (calcd), g/cm ³	1.55
<i>V</i> , Å ³	3302.2		
diffractometer	Enraf-Nonius CAD4	reflecons collected	3586
radiation	Mo Kα	unique reflecons	2500
wavelength, Å	0.71073	unique reflecons with <i>F</i> ₀ ≥ 5σ(<i>F</i> ₀)	2107
scan method	ω-θ		
max 2θ, deg	50.0		
scan speed	2-20 (in ω)		
deg/min			
<i>R</i> (int), % ^a	2.92		
<i>R</i> _F , <i>R</i> _{wF} , % ^b	4.9, 5.7	Δ/σ (final)	0.003
GOF ^c	1.228	Δ(ρ), e/Å ³	1.29
data/parameter	11.1		

^a *R*(int) = [Σ{*N*Σ[w(*F*(mean) - *F*)²]} / Σ{(*N* - 1)Σ[w*F*²]}]^{1/2}. ^b *R*_F = Σ|Δ| / Σ|*F*₀| and *R*_{wF} = Σ(|Δ|w^{1/2}) / Σ(|*F*₀|w^{1/2}), where Δ = |*F*_o| - |*F*_c|. ^c GOF = [Σw(Δ)² / (*N*_{observns} - *N*_{params})]^{1/2}.

NMe₃·2H₂O by the reported procedure.⁴ Infrared spectra were recorded on either a IBM FTIR/32 or FTIR/85 spectrometer. Proton and ¹³C NMR spectra were determined on a Varian XL-200 spectrometer.

Preparation of [Na(18-crown-6)][W(CO)₅CH₃]. A solution of W(CO)₅NMe₃ (0.73 g (1.9 mmol) in 30 mL of THF) cooled to -78 °C was titrated with sodium naphthalenide (0.14 M in THF) until the green color persisted, generating Na₂W(CO)₅. Methyl *p*-toluenesulfonate (0.4 mL (2.4 mmol)) was added to the solution maintained at -78 °C, and the solution was stirred for 20 min. Following this period the reaction solution was allowed to warm slowly to ambient temperature and filtered. A solution of 18-crown-6 (0.603 g (2.28 mmol) in 5.0 mL of THF) was added to the filtrate, and the solution was stirred overnight. Upon addition of hexane a pale yellow powder precipitated from solution which was isolated by filtration. Crystals suitable for X-ray analysis were grown from THF/hexane (1:2 by volume) at 0 °C. Infrared spectrum (ν(CO) region, in THF): 2030.3 (w), 1882.8 (s), 1835.5 (m) cm⁻¹. ¹H NMR

- (1) Darensbourg, D. J.; Kudarski, R. *J. Am. Chem. Soc.* **1984**, *106*, 3672.
- (2) Darensbourg, D. J.; Hanckel, R. K.; Bauch, C. G.; Pala, M.; Simmons, D.; White, J. N. *J. Am. Chem. Soc.* **1985**, *107*, 7463.
- (3) Darensbourg, D. J.; Grottsch, G. *J. Am. Chem. Soc.* **1985**, *107*, 7473.
- (4) Cooper, N. J.; Maher, J. N.; Beatty, R. P. *Organometallics* **1982**, *1*, 215.

* To whom correspondence should be addressed.

† Texas A&M University.

‡ University of Delaware.

Table II. Atomic Coordinates ($\times 10^4$) and Isotropic Thermal Parameters ($\text{\AA}^2 \times 10^3$)

	<i>x</i>	<i>y</i>	<i>z</i>	<i>U</i> ^a
W	0	1067 (1)	7500	37 (1)
Na	5000	0	10000	43 (2)
O(1)	0	3556 (7)	7500	63 (4)
O(2)	702 (6)	604 (7)	8982 (4)	69 (3)
O(3)	2345 (6)	1360 (7)	7115 (4)	75 (3)
O(4)	4804 (5)	1561 (5)	9051 (3)	40 (2)
O(5)	6189 (4)	1844 (5)	10139 (3)	39 (2)
O(6)	6031 (4)	425 (5)	11173 (3)	38 (2)
O(7)	3568 (5)	745 (6)	10495 (3)	58 (3)
C(1)	0	2633 (12)	7500	48 (5)
C(2)	456 (7)	844 (7)	8455 (4)	37 (3)
C(3)	1471 (9)	1168 (8)	7281 (4)	47 (3)
C(4)	0	-769 (13)	7500	85 (8)
C(5)	5601 (8)	2332 (8)	9069 (5)	49 (3)
C(6)	5782 (8)	2698 (8)	9761 (5)	50 (3)
C(7)	6404 (7)	2155 (7)	10798 (4)	46 (3)
C(8)	6808 (7)	1223 (7)	11183 (4)	45 (3)
C(9)	6287 (8)	-444 (8)	11595 (4)	49 (3)
C(10)	5391 (7)	-1182 (8)	11601 (4)	46 (3)
C(11)	3541 (11)	1355 (17)	11050 (9)	151 (10)
C(12)	2583 (11)	1435 (14)	11325 (8)	110 (7)
C(13)	1903 (11)	1034 (18)	10808 (10)	159 (12)
C(14)	2548 (11)	588 (17)	10304 (10)	149 (9)

^a Equivalent isotropic *U* defined as one-third of the trace of the orthogonalized U_{ij} tensor.

(CD_2Cl_2): δ -0.762 (s, 3 H), 3.708 (s, 24 H). ^{13}C NMR (CD_2Cl_2): δ -34.21 (s, CH_3), 89.57 (s, $-\text{CH}_2\text{CH}_2-$), 207.2 (s, cis CO), 210.4 (s, trans CO).

X-ray Crystallographic Study of $[\text{Na}(\text{18-crown-6})(\text{THF})_2][\text{W}(\text{CO})_5\text{CH}_3]$. Data Collection and Reduction. A yellow platelike crystal of $\text{C}_{26}\text{H}_{45}\text{O}_{13}\text{NaW}$ having approximate dimensions of $0.20 \times 0.15 \times 0.08$ mm was mounted on a glass fiber in a random orientation. Preliminary examination and data collection were performed on a computer-controlled κ -axis diffractometer equipped with a graphite-crystal, incident-beam monochromator. The scan rate varied from 2 to $20^\circ/\text{min}$ (in ω). The variable scan rate allows rapid data collection for intense reflections, where fast scan rate is used, and assures good counting statistics for weak reflections, where a slow scan rate is used. Data were collected to a maximum 2θ value of 50° . The scan range (in degrees) was determined as a function of θ to correct for the separation of the $K\alpha$ doublet. The scan width was calculated as follows: θ scan width = $0.7 + 0.350 \tan \theta$. Moving-crystal-moving-counter background counts were made by scanning an additional 25% above and below the range. Thus the ratio of peak aperture was also adjusted as a function of θ . The horizontal aperture width ranged from 2.0 to 2.5 mm; the vertical aperture was set at 2.0 mm. The diameter of the incident-beam collimator was 0.7 mm, and the crystal to detector distance was 21 cm. For intense reflections an attenuator was automatically inserted in front of the detector; the attenuator factor was 20.7. A total of 3186 reflections were collected. As a check on crystal and electronic stability three representative reflections were measured every 41 min. Lorentz and polarization corrections were applied to the data. A series of ψ scans were collected.

Structure Solution and Refinement. Systematic absences in the intensity data indicated either of the monoclinic space groups $C2/c$ or Cc . The centrosymmetric alternative, $C2/c$, was initially assumed and later proved correct by the chemically reasonable, well-behaved solution and refinement of the structure. The W atom was located by a Patterson synthesis, and the remaining non-hydrogen atoms were found from subsequent difference Fourier maps. The asymmetric unit consists of half of the $[\text{Na}(\text{18-crown-6})(\text{THF})_2]^+$ cation with Na situated at an inversion center and half of the $\text{W}(\text{CO})_5\text{CH}_3^-$ anion with the C(4)-W-C(1)-O(1) axis coinciding with a twofold rotational axis.

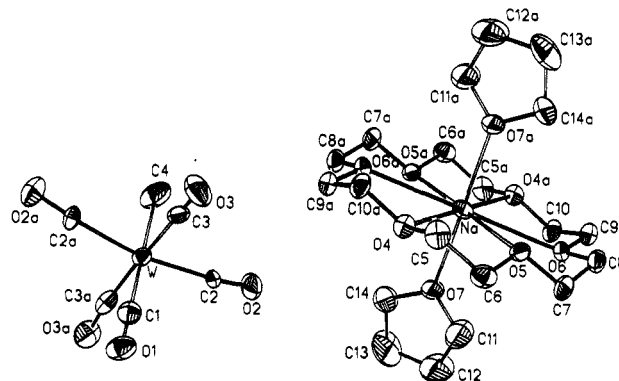
Block-cascade refinement used a model with all non-hydrogen atoms anisotropic, and all hydrogen atoms (except for the C(4) methyl group) were included as idealized, updated isotropic contributions ($d(\text{C}-\text{H}) = 0.96 \text{ \AA}$). Atomic coordinates are given in Table II and selected bond distances and angles in Tables III and IV, respectively. Additional crystallographic data are available as supplementary data. All computer programs are contained in the SHELXTL (version 5.1) program library (Nicolet Corp., Madison, WI).

Table III. Bond Lengths (\AA)

W-C(1)	1.975 (15)	W-C(2)	2.022 (8)
W-C(3)	1.975 (11)	W-C(4)	2.313 (17)
W-C(2A)	2.022 (8)	W-C(3A)	1.975 (11)
Na-O(4)	2.755 (6)	Na-O(5)	2.798 (6)
Na-O(6)	2.739 (6)	Na-O(7)	2.333 (7)
Na-O(4A)	2.755 (6)	Na-O(5A)	2.798 (6)
Na-O(6A)	2.740 (6)	Na-O(7A)	2.333 (7)
O(1)-C(1)	1.164 (8)	O(2)-C(2)	1.143 (11)
O(3)-C(3)	1.215 (13)	O(4)-C(5)	1.418 (12)
O(4)-C(10A)	1.419 (10)	O(5)-C(6)	1.412 (11)
O(5)-C(7)	1.409 (10)	O(6)-C(8)	1.423 (11)
O(6)-C(9)	1.422 (12)	O(7)-C(11)	1.361 (20)
O(7)-C(14)	1.380 (16)	C(5)-C(6)	1.485 (14)
C(7)-C(8)	1.496 (13)	C(9)-C(10)	1.488 (14)
C(10)-O(4A)	1.419 (10)	C(11)-C(12)	1.381 (21)
C(12)-C(13)	1.439 (23)	C(13)-C(14)	1.452 (26)

Table IV. Bond Angles

C(1)-W-C(2)	98.0 (2)	C(1)-W-C(3)	86.3 (3)
C(2)-W-C(3)	88.1 (3)	C(1)-W-C(4)	180.0 (1)
C(2)-W-C(4)	82.0 (2)	C(3)-W-C(4)	93.7 (3)
C(1)-W-C(2A)	98.0 (2)	C(2)-W-C(2A)	164.0 (5)
C(3)-W-C(2A)	92.9 (3)	C(4)-W-C(2A)	82.0 (2)
C(1)-W-C(3A)	86.3 (3)	C(2)-W-C(3A)	92.9 (3)
C(3)-W-C(3A)	172.5 (6)	C(4)-W-C(3A)	93.7 (3)
O(4)-Na-O(5)	61.0 (2)	O(4)-Na-O(6)	119.7 (2)
O(5)-Na-O(6)	59.9 (2)	O(4)-Na-O(7)	87.3 (2)
O(5)-Na-O(7)	93.8 (2)	O(6)-Na-O(7)	85.6 (2)
O(4)-Na-O(4A)	180.0 (1)	O(5)-Na-O(4A)	119.0 (2)
O(6)-Na-O(4A)	60.3 (2)	O(7)-Na-O(4A)	92.7 (2)
O(4)-Na-O(5A)	119.0 (2)	O(5)-Na-O(5A)	180.0 (1)
O(6)-Na-O(5A)	120.1 (2)	O(7)-Na-O(5A)	86.3 (2)
O(4)-Na-O(6A)	60.3 (2)	O(5)-Na-O(6A)	120.1 (2)
O(6)-Na-O(6A)	180.0 (1)	O(7)-Na-O(6A)	94.4 (2)
O(4)-Na-O(7A)	92.7 (2)	O(5)-Na-O(7A)	86.3 (2)
O(6)-Na-O(7A)	94.4 (2)	O(7)-Na-O(7A)	180.0 (1)
Na-O(4)-C(5)	114.9 (5)	Na-O(4)-C(10A)	114.6 (5)
C(5)-O(4)-C(10A)	111.3 (7)	Na-O(5)-C(6)	112.6 (5)
Na-O(5)-C(7)	114.7 (5)	C(6)-O(5)-C(7)	111.0 (7)
Na-O(6)-C(8)	118.5 (5)	Na-O(6)-C(9)	117.9 (5)
C(8)-O(6)-C(9)	112.6 (7)	Na-O(7)-C(11)	128.5 (7)
Na-O(7)-C(14)	126.1 (9)	C(11)-O(7)-C(14)	105.3 (11)
W-C(1)-O(1)	180.0 (1)	W-C(2)-O(2)	172.7 (8)
W-C(3)-O(3)	171.6 (8)	O(4)-C(5)-C(6)	109.3 (8)
O(5)-C(6)-C(5)	108.5 (8)	O(5)-C(7)-C(8)	109.2 (7)
O(6)-C(8)-C(7)	108.2 (7)	O(6)-C(9)-C(10)	108.6 (7)
C(9)-C(10)-O(4A)	108.6 (7)	O(7)-C(11)-C(12)	114.8 (13)
C(11)-C(12)-C(13)	102.7 (14)	C(12)-C(13)-C(14)	107.0 (12)
O(7)-C(14)-C(13)	108.4 (15)		

**Figure 1.** Ion structures and labeling scheme for $[\text{Na}(\text{18-crown-6})(\text{THF})_2][\text{W}(\text{CO})_5\text{CH}_3]$ as paired in the lattice.

Results and Discussion

Crystal and Molecular Structure of $[\text{Na}(\text{18-crown-6})(\text{THF})_2][\text{W}(\text{CO})_5\text{CH}_3]$. The final atomic coordinates for all non-hydrogen atoms of both the cation and anion are provided in Table II. The anisotropic thermal parameters for all non-

(5) These services were performed by the crystallographic staff of Molecular Structure Corp.: Dr. M. W. Extine, Dr. W. Pennington, Dr. P. N. Swebston, Dr. J. M. Troup, and B. B. Warrington.

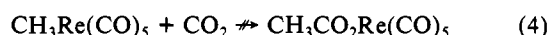
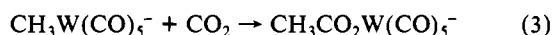
hydrogen atoms and the calculated atomic coordinates for the hydrogen atoms in crystalline [Na(18-crown-6)(THF)₂][W(CO)₅CH₃] are available as supplementary material. Bond lengths and bond angles for both the anion and cation are presented in Tables III and IV. The structure of the title compound consists of an array of the two discrete ionic units, at normal van der Waals distances (Figure in supplementary material). The three-dimensional structure of the cation and anion is shown in Figure 1, which illustrates that the sodium ion is octacoordinated and the tungsten metal is in an octahedral environment.

The 18-crown-6 macrocycle adopts an approximately planar arrangement of oxygen atoms in which the sodium ion is centrally located at a nonoptimum distance of 2.75 Å.^{6a} The six oxygen atoms alternate above and below the plane of best fit with a maximum deviation of 0.174 Å. This is the standard crown configuration for Na⁺ or K⁺.^{6b} The coordination geometry about the sodium ion is that of a slightly distorted hexagonal bipyramid with the oxygen atoms of THF molecules occupying the two axial coordinated sites. Alternatively, the coordination geometry about the sodium ion may be described as an axially bicapped trigonal antiprism. The Na–O distances in the macrocycle complex are in the range 2.739 (6)–2.798 (6) Å, with an average distance of 2.764 (6) Å. The Na–O distances to the two axial tetrahydrofuran molecules are much shorter at 2.333 (7) Å.

The distribution of the ligands about the tungsten metal center is that of a distorted octahedron, where the average OC(ax)–W–CO(eq) angle is 92.2°. Two of the equatorial CO ligands (mutually trans to one another) are bent toward the methyl group (OC(eq)–W–CH₃ = 82°), whereas the other two equatorial CO ligands bend away from the alkyl ligand (93.7°). The average W–CO(eq) distance is 1.999 (10) Å while the axial W–CO bond length is 1.975 (15) Å. Hence, the methyl group, located 2.313 (17) Å from the tungsten metal center, does not exert a significant trans effect. This is in marked contrast to the case for the acetate ligand, the product of CO₂ insertion into the W–CH₃ linkage, where the shortening of the axial M–CO bond distance over the equatorial M–CO bond distance is 0.087 Å.⁷

We now wish to focus on the major reasons for carrying out a low-temperature X-ray structural analysis of the salt containing the CH₃W(CO)₅[−] anion, and its phosphine-substituted analogue *cis*-CH₃W(CO)₄PMe₃[−], that is, the W–CH₃ bonding parameters. The W–CH₃ bond distance in CH₃W(CO)₅[−] at 2.313 (17) Å is almost identical with the Re–CH₃ bond length observed in the isoelectronic neutral analogue CH₃Re(CO)₅, where a Re–CH₃ bond distance of 2.308 (17) Å has been determined by electronic diffraction methods.⁸ Other similarities noted in the two structures include the average Re–CO bond distances (2.000 (4) Å) and OC(eq)–M–CO(ax) bond angles (96 (2)°).

The resemblance of the M–CH₃ bonds in CH₃W(CO)₅[−] and CH₃Re(CO)₅ presumably holds as well with regard to their bond energies. The dissociation energy for the rhenium–methyl carbon bond in CH₃Re(CO)₅ has been reported as being 222 kJ mol^{−1}.⁹ This is an interesting comparison in that there is a large discrepancy in the reactivities of these two metal alkyls toward CO₂ insertion reactions. That is, whereas reaction 3 occurs under moderate conditions, reaction 4 has not been observed to occur



under more rigorous conditions. The difference in reactivity is thereby assumed to be a consequence of the enhanced interaction of carbon dioxide with a more electron-rich metal center, that is,

Table V. Second-Order Rate Constants for Carbon Dioxide Insertion into *cis*-CH₃W(CO)₄L[−] Derivatives^a

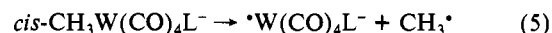
L	k ₂ , s ^{−1} M ^{−1}	rel rates
CO	3.46 × 10 ^{−6}	1
P(OMe) ₃	2.00 × 10 ^{−4}	57.8
PMe ₃	8.40 × 10 ^{−4}	243

^a Reactions carried out in tetrahydrofuran at 25 °C at a carbon dioxide pressure of 760 torr with the PPN⁺ salts. Results taken from ref 2.

metal–CO₂ bond making offsets metal–alkyl bond breaking.

The effect of an increase in electron density at the metal center on the rate of CO₂ insertion into metal–carbon bonds is dramatically demonstrated as well when CO is replaced in the metal's coordination sphere by phosphorus donor ligands. A systematic increase in the rate of carbon dioxide insertion into the W–CH₃ bond has been noted with increasing phosphorus ligand donicity (Table V).² This was ascribed to an increase in carbon dioxide interaction at the metal center and not due to a weakening of the metal–carbon bond. The W–CH₃ bond distance in *cis*-CH₃W(CO)₄PMe₃[−] (2.18 (3) Å) as compared with that determined herein for CH₃W(CO)₅[−] (2.313 (17) Å) supports this assumption. Because of the sizable esd's in these bond parameters it is not possible to accurately assess the degree of bond stabilization upon phosphine substitution; it is, however, clear that the W–CH₃ bond is stabilized by the more electron-rich metal center.

The stabilization of the W–CH₃ bond manifested in the CH₃W(CO)₅[−] anion by, replacing one CO ligand with PMe₃ can be understood in terms of the process defined specifically in eq 5. That is, dissociation of the W–CH₃ bond implies a decrease



in the formal oxidation state of tungsten, proceeding from W(0) to W(−1). More electron donating ligands (L) favor the higher oxidation state and hence stabilize the tungsten–alkyl derivative and inhibit W–CH₃ bond homolysis. This phenomenon has previously been elegantly discussed for Co–C bond dissociation processes.¹⁰ Concomitantly, the sensitivity of the Co–R bond dissociation energy to steric effect has been noted;¹⁰ hence, it is important that we limit our conclusions to spatially small L ligands.

Solution Structure of [Na(18-crown-6)][CH₃W(CO)₅]. The title complex exists in tetrahydrofuran solution as solvent-separated ion pairs or free ions.¹¹ This is readily assessed by noting the similarity of the ν(CO) spectra of the CH₃W(CO)₅[−] anion in the presence of either PPN⁺ (2028 (w), 1883 (s), and 1834 (m) cm^{−1}) or Na(18-crown-6)⁺ (2030 (w), 1883 (s), and 1836 (m) cm^{−1}). Hence, the solution structure is much like the solid-state structure, consisting of isolated anions and cations.

The reactivity of [Na(18-crown-6)(THF)₂][CH₃W(CO)₅] in THF with carbon dioxide to afford the acetate complex is the same as that of [Na(THF)_n][CH₃W(CO)₅] and about 1 order of magnitude greater than that of the salts of the noninteracting counterions PPN⁺ and Na(Kryptofix-221)⁺.¹² This rate enhancement has been ascribed to the sodium cation's ability to neutralize the buildup of negative charge on the incipient carboxylate ligand. Indeed, in both the Na(THF)_n⁺ and Na(18-crown-6)⁺ derivatives perturbation of the once-formed acetate ligand by Na⁺ has been noted spectroscopically. This interaction occurs via contact-ion pairing of the Na⁺ ion with the distal, very basic oxygen atom of the acetate ligand, an interaction that has been observed even in the solid state with Na⁺ encapsulated by Kryptofix-221.¹²

Therefore, it is evident from these rate studies that the coordination of THF solvent molecules at the axial sites in the Na(18-crown-6)⁺ cation is a dynamic process. That is, these ligands are easily displaced from Na⁺ as the more basic carboxylate site becomes available in the metal's coordination sphere. We are

- (6) (a) Dunitz, J. D.; Dobler, M.; Seiler, P.; Rhizackerley, R. P. *Acta Crystallogr., Sect. B: Struct. Crystallogr. Cryst. Chem.* **1974**, *B30*, 2377. (b) Dale, J. *Isr. J. Chem.* **1980**, *20*, 3.
 (7) Cotton, F. A.; Darensbourg, D. J.; Kolthammer, B. W. S.; Kudarski, R. *Inorg. Chem.* **1982**, *21*, 1656.
 (8) Rankin, D. W. H.; Robertson, A. *J. Am. Chem. Soc.* **1976**, *105*, 331.
 (9) Brown, D. L. S.; Connor, J. A.; Skinner, H. A. *J. Organomet. Chem.* **1974**, *81*, 403.

- (10) Halpern, J. *Acc. Chem. Res.* **1982**, *15*, 238 and references therein.
 (11) Darensbourg, M. Y. *Prog. Inorg. Chem.* **1985**, *33*, 221 and references therein.
 (12) Darensbourg, D. J.; Pala, M. *J. Am. Chem. Soc.* **1985**, *107*, 5687.

currently attempting to obtain X-ray-quality crystals of $[\text{Na}(18\text{-crown-6})][\text{CH}_3\text{CO}_2\text{W}(\text{CO})_3]$ in an effort to better define this interaction. Further, we hope to analyze crystals of $[\text{Na}(18\text{-crown-6})][\text{cis-CH}_3\text{W}(\text{CO})_4\text{PMe}_3]$, where it is expected that the possibility of observing Na^+ interaction at the more basic oxygen sites of the carbonyl ligands is greatly enhanced.

Acknowledgment. The financial support of this research by the

National Science Foundation (Grant CHE 86-03681) is greatly appreciated.

Supplementary Material Available: Stereoview of the unit cell packing for $[\text{Na}(18\text{-crown-6})(\text{THF})_2][\text{W}(\text{CO})_5\text{CH}_3]$ and tables of anisotropic thermal parameters and derived atomic coordinates for hydrogen atoms (3 pages); a table of calculated and observed structure factors (13 pages). Ordering information is given on any current masthead page.

Contribution from the Department of Chemistry,
University of South Carolina, Columbia, South Carolina 29208

Cluster Condensation Reactions. Transformation of Two Triangular Trinuclear Clusters into a Hexanuclear Cluster Containing a Novel *Edge-Fused* Bitetrahedral Structure

Richard D. Adams* and James E. Babin

Received September 4, 1986

The carbene-containing cluster complex $\text{Os}_3(\text{CO})_9[\text{C}(\text{H})\text{NMe}_2](\mu\text{-SMe})(\mu\text{-H})$ (**1**) was prepared in 56% yield from the reaction of $\text{Os}_3(\text{CO})_{10}(\mu\text{-SMe})(\mu\text{-H})$ with $\text{CH}_2(\text{NMe}_2)_2$. UV irradiation of **1** yielded the complex $\text{Os}_3(\text{CO})_8(\mu\text{-CNMe}_2)(\mu\text{-SMe})(\mu\text{-H})_2$ (**2**) in 68% yield. Compound **2** contains a bridging (dimethylamino)carbyne ligand that was formed by an $\alpha\text{-CH}$ activation of the carbene ligand in **1**. Thermal decarbonylation of **2** resulted in the formation of the hexaosmium cluster complex $\text{Os}_6(\text{CO})_{12}(\mu\text{-CNMe}_2)_2(\mu_3\text{-SMe})_2(\mu\text{-H})_2$ (**3**) in 65% yield. Compound **3** was characterized by a single-crystal X-ray diffraction analysis. Crystal data: space group $P2_1/c$, $a = 16.042$ (4) Å, $b = 12.670$ (3) Å, $c = 17.816$ (3) Å, $\beta = 101.59$ (2)°, $Z = 4$, $\rho_{\text{calcd}} = 3.23$ g/cm³. The structure was solved by a combination of direct methods and difference Fourier techniques and was refined (2701 reflections) to the final values of the residuals $R = 0.048$ and $R_w = 0.050$. The structure consists of six osmium atoms arranged in the form of two tetrahedral clusters that have one edge in common. There are two bridging (dimethylamino)carbyne ligands and two triply bridging methanethiolato ligands that appear to serve as three-electron donors instead of the usual five-electron-donor configuration.

Introduction

The development of systematic routes for their syntheses has been one of the greatest challenges to researchers investigating the chemistry of transition-metal cluster compounds.¹⁻³ In our recent studies we have focused on the ability of sulfido ligands in metal complexes to facilitate cluster synthesis.^{1,4} In related work we have been investigating the synthesis and transformation behavior of heteronuclear carbene ligands in cluster compounds.⁵ We have now found that decarbonylation of the compound $\text{Os}_3(\text{CO})_8(\mu\text{-CNMe}_2)(\mu\text{-SMe})(\mu\text{-H})_2$ results in the formation of the hexanuclear product $\text{Os}_6(\text{CO})_{12}(\mu\text{-CNMe}_2)_2(\mu_3\text{-SMe})_2(\mu\text{-H})_2$ with a cluster that consists of a pair of fused tetrahedra that has a pair of unusually coordinated triply bridging methanethiolato ligands. The thiolato ligands are believed to have played an important role in the formation of this hexanuclear product. The results of these studies are described in this report.

Experimental Section

General Procedures. Although all the products appear to be air stable, all the reactions were performed in the standard Schlenkware under a dry nitrogen atmosphere, unless otherwise specified. Reagent grade solvents were dried over molecular sieves and deoxygenated by purging with nitrogen prior to use. The compound $\text{Os}_3(\text{CO})_9[\text{C}(\text{H})\text{NMe}_2](\mu\text{-SMe})(\mu\text{-H})$ (**1**) was obtained in 56% yield from the reaction of $\text{Os}_3(\text{CO})_{10}(\mu\text{-SMe})(\mu\text{-H})$ ⁶ and $\text{CH}_2(\text{NMe}_2)_2$ according to a procedure that was analogous to that which was used for the preparation of the arene-thiolato analogue of **1**.⁵ For **1**: IR ($\nu(\text{CO})$ cm⁻¹ in hexane) 2091 (m), 2051 (s), 2012 (vs), 2006 (m), 2001 (s), 1964 (m), 1938 (w); ¹H NMR

(δ in CDCl_3) 11.69 (s, 1 H), 3.61 (s, 3 H), 3.57 (s, 3 H), 2.38 (s, 3 H), -17.51 (s, 1 H). Anal. Calcd for **1**: C, 16.80; N, 1.51; H, 1.20. Found: C, 17.01; N, 1.54; H, 1.11. Photolysis experiments were performed by using an externally positioned high-pressure mercury lamp on reaction solutions contained in Pyrex glassware. IR spectra were recorded on a Nicolet 5DXB FTIR spectrophotometer. A Bruker AM300 FT-NMR spectrometer was used to obtain ¹H NMR spectra. Elemental analyses were performed by MICANAL, Tucson, AZ.

Photolysis of $\text{Os}_3(\text{CO})_9[\text{C}(\text{H})\text{NMe}_2](\mu\text{-SMe})(\mu\text{-H})$ (1**).** A cyclohexane solution (50 mL) of **1** (25 mg, 0.0027 mmol) was subjected to UV irradiation for 45 min in the presence of a continuous purge with nitrogen. The solvent was removed in vacuo. The residue was extracted with a minimum of CH_2Cl_2 and was chromatographed by TLC on silica gel. Elution with a 30%/70% CH_2Cl_2 /hexane solvent mixture yielded the yellow product $\text{Os}_3(\text{CO})_8(\mu\text{-CNMe}_2)(\mu\text{-SMe})(\mu\text{-H})_2$ (**2**) (17 mg, (68% yield)). IR ($\nu(\text{CO})$ cm⁻¹ in hexane): 2085 (m), 2048 (vs), 2018 (s), 2012 (s), 1990 (m), 1974 (m), 1951 (m). ¹H NMR (δ , in CDCl_3 solvent): 3.99 (s, 3 H), 3.87 (s, 3 H), 2.58 (s, 3 H), -13.91 (s, 1 H), -15.95 (s, 1 H).

Thermolysis of **2.** An octane solution (40 mL) of **2** (20 mg, 0.223 mmol) was refluxed for 90 min. The solvent was removed in vacuo, and the product was isolated by TLC on silica gel. Elution with a 40%/60% CH_2Cl_2 /hexane solvent mixture yielded red $\text{Os}_6(\text{CO})_{12}(\mu\text{-CNMe}_2)_2(\mu_3\text{-SMe})_2(\mu\text{-H})_2$ (**3**) (13 mg (65%)). IR ($\nu(\text{CO})$ cm⁻¹ in hexane) for **3**: 2042 (w), 2018 (s), 1998 (vs), 1989 (s), 1961 (m), 1950 (m), 1939 (w). ¹H NMR at 25 °C (δ , in CDCl_3 solvent): 3.81 (s, 12 H), 3.12 (s, 6 H), -15.80 (s, 2 H). ¹H NMR at -80 °C (δ , in CD_2Cl_2 solvent): 3.84 (s, 6 H), 3.79 (s, 6 H), 3.15 (s, 6 H), -15.77 (s, 2 H).

Crystallographic Analysis. Red crystals of **3** were grown by slow evaporation of solvent from CH_2Cl_2 /hexane solutions at -20 °C. The data crystal was mounted in a thin-walled glass capillary. Diffraction measurements were made on a Rigaku AFC6 automatic diffractometer by using $\text{Mo K}\alpha$ radiation. The unit cell for **3** was determined by using the AFC6 automatic search, index, center, and least-squares routines. Crystal data, data collection parameters, and results of the analysis are listed in Table I. Data processing was performed on a Digital Equipment Corp. MICROVAX I computer by using the TEXSAN structure solving program library obtained from the Molecular Structure Corp., College Station, TX. An absorption correction of a Gaussian integration type was performed. Neutral-atom scattering factors were calculated by the standard procedures.^{7a} Anomalous dispersion corrections were applied

- (1) Adams, R. D. *Polyhedron* **1985**, *4*, 2003.
- (2) Vahrenkamp, H. *Philos. Trans. R. Soc. London, A* **1982**, *308*, 17.
- (3) Vahrenkamp, H. *Adv. Organomet. Chem.* **1983**, *22*, 169.
- (4) Adams, R. D.; Dawoodi, Z.; Foust, D. F.; Segmuller, B. *J. Am. Chem. Soc.* **1983**, *105*, 831.
- (5) (a) Adams, R. D.; Babin, J. E.; Kim, H. S. *Organometallics* **1986**, *5*, 1924. (b) Adams, R. D.; Babin, J. E.; Kim, H. S. *J. Am. Chem. Soc.*, in press.
- (6) Crooks, G. R.; Johnson, B. F. G.; Lewis, J.; Williams, I. G. *J. Chem. Soc. A* **1969**, 797.